Concentration and Molecular Weight Dependence of Viscoelastic Properties in Linear and Star Polymers

V. R. Raju,* E. V. Menezes,† G. Marin,‡ and W. W. Graessley

Chemical Engineering and Materials Science Departments, Northwestern University, Evanston, Illinois 60201

L. J. Fetters

The Institute of Polymer Science, University of Akron, Akron, Ohio 44325.
Received May 7, 1981

ABSTRACT: Superposition principles have been applied to the dynamic moduli, $G'(\omega)$ and $G''(\omega)$, of five species of linear polymers and their concentrated solutions to establish forms for the terminal response in the limit of long chains and high concentrations. Below ω_m, the frequency at which the loss modulus assumes its maximum value G_m'', reduced curves of $G'(\omega)/G_m''$ and $G''(\omega)/G_m''$ vs. ω/ω_m settle into limiting forms rather quickly ($M \gtrsim 5M_e$, where M_e is the entanglement molecular weight). Above ω_m the approach is slower, and $M \gtrsim 100M_e$ appears necessary to fully resolve the terminal response from plateau and transition contributions. The limiting forms are tabulated and used to derive "universal" values of the viscoelastic property combinations $G_N^0 J_e^0 = 2.40$, $\eta_0\omega_m/G_N^0 = 0.97$, and $G_m''/G_N^0 = 3.56$ for linear entangled polymers with very narrow chain length distributions. Dynamic moduli for star polymers at different concentrations were also found to be superposable. The reduced curves change with chain structure, however, and the universality suggested for entangled linear chain systems seems not applicable for entangled stars. Some interesting properties for stars are observed nonetheless. The modulus shift factor is directly proportional to polymer concentration, and the values of recoverable compliance J_e^0 are in remarkable agreement with those calculated from the Rouse–Ham theory.

Introduction

The linear viscoelastic properties of narrow-distribution polymers at high concentrations have been the subject of numerous studies.[1,2] Separation of the relaxation spectrum $H(\tau)$ into distinct terminal and transition regions for linear chain systems is well established. The separation first appears when the molecular weight M exceeds M_c, the characteristic molecular weight for zero shear viscosity η_0 at that concentration, and then increases rapidly with increasing chain length. Moreover, the behavior of the plateau modulus G_N^0 and the steady-state recoverable compliance J_e^0 suggests a remarkable similarity in the form of the terminal spectrum $H_1(\tau)$ for different polymer species. For $M \gg M_c$, these quantities and the viscosity can be expressed as moments of the terminal relaxation spectrum alone:[2]

$$G_N^0 = \int_{-\infty}^{\infty} H_1(\tau)\, d \ln \tau \tag{1}$$

$$\eta_0 = \int_{-\infty}^{\infty} \tau H_1(\tau)\, d \ln \tau \tag{2}$$

$$J_e^0 = \frac{1}{\eta_0^2}\int_{-\infty}^{\infty} \tau^2 H_1(\tau)\, d \ln \tau \tag{3}$$

The product $G_N^0 J_e^0$ is therefore a measure of the breadth of the terminal spectrum

$$G_N^0 J_e^0 = \frac{\int_{-\infty}^{\infty} \tau^2 H_1(\tau)\, d \ln \tau \Big/ \int_{-\infty}^{\infty} \tau H_1(\tau)\, d \ln \tau}{\int_{-\infty}^{\infty} \tau H_1(\tau)\, d \ln \tau \Big/ \int H_1(\tau)\, d \ln \tau} = \frac{\langle \tau \rangle_w}{\langle \tau \rangle_n} \tag{4}$$

and practically the same value, $G_N^0 J_e^0 = 3.0 \pm 0.5$, is found for different polymer species. The product is independent of molecular weight M (for $M \gg M_c$) and the temperature T. It is also independent of polymer volume fraction ϕ and diluent species in concentrated solutions,[2,3] again for sufficiently long chains. From these results, the terminal spectrum breadth appears to be effectively universal.

In this paper we use superposition principles to establish more detailed information on the form of the terminal spectrum in the long-chain limit. The terminal response is separated from overlapping processes (the plateau and transition responses) by using data on the dynamic moduli, $G'(\omega)$ and $G''(\omega)$, for several linear species at various molecular weights and concentrations. Superposition of dynamic moduli for star-branched polymers at different concentrations is also examined.

Experimental Samples and Procedures

Six structural species prepared by anionic polymerization are represented: linear polybutadiene (designated by L),[3,4] fully hydrogenated linear polybutadiene (designated by HPB or PHPB),[5] polybutadiene stars (designated by S),[3] linear polystyrene (designated by C),[6] linear polyisoprene (designated by PI),[7] and fully hydrogenated polyisoprene (designated by HPI).[7] Hydrogenated linear polybutadiene has the polyethylene structure except that it contains ~18 ethyl branches/1000 backbone carbon atoms. It is virtually indistinguishable from linear polyethylene in the melt state.[5] Hydrogenated polyisoprene is equivalent to a strictly alternating copolymer of ethylene and propylene although it contains about 20 isopropyl side branches/1000 backbone carbon atoms.[7] All samples have narrow molecular weight distributions ($\bar{M}_w/\bar{M}_n < 1.1$). Molecular characterization data are given in Table I.

The diluents used for polybutadiene are listed in Table II. The first four are commercial hydrocarbon oils. Tetradecane is a good solvent for polybutadiene, isobutyl acetate is a Θ solvent (Θ ≈ 20 °C), and chain dimensions with the low molecular weight polybutadiene as solvent should be near the unperturbed values. Glass temperatures for the solvents range from well below to well above $T_g = -95$ °C for high molecular weight polybutadiene. Two low molecular weight linear polyethylenes with narrow distributions (Bareco waxes, Petrolite Corp.) were used as diluents for the hydrogenated polybutadienes (see Table I).

The polybutadiene solutions were prepared by dissolving the diluent and polymer in an excess of benzene and then stripping out the benzene under vacuum at 25 °C.[3] The hydrogenated

*Present address: Bell Laboratories, Murray Hill, NJ 07974.
†Present address: Ethicon, Inc., Somerville, NJ 08876.
‡Present address: Laboratoire de Thermodynamique, Université de Pau, F-64000 Pau, France.

0024-9297/81/2214-1668$01.25/0

Table I
Molecular Characteristics of Polymers Included in This Study

sample	$(\bar{M}_w)_{GPC} \times 10^{-4}$	$(\bar{M}_w/\bar{M}_n)_{GPC}$	M/M_e	$[\eta]_{THF}$, dL/g
L3	0.46	<1.05	2.4	0.11
L200	20.0	<1.05	105	2.10
L230	23.0	<1.05	121	2.21_5
L340	34.0	<1.05	179	3.15
L350	35.0	<1.05	184	3.18_5
L500	51.7	<1.05	272	4.63_5
L780	81.3	<1.05	428	6.15
S100[a]	9.9	<1.05	52	1.00[d]
S200[b]	19.2	<1.05	101	1.40[d]
PI-1	13.2	<1.05	21	0.99
HPI-1	13.3	<1.05	67	1.27
C6bb	27.5	<1.05	17	
C7bb	86.0	<1.05	52	

sample	$\bar{M}_w \times 10^{-4}$ [c]	$(\bar{M}_w/\bar{M}_n)_{GPC}$	M/M_e	$[\eta]_{TCB}$, dL/g
HPB-230	21.2	<1.05	177	2.76
HPB-350	35.9	<1.05	300	4.02
PHPB-4	17.4		145	2.41
PHPB-5	22.9		190	2.92
Bareco 1000	0.12	<1.20	1.0	0.07_5
Bareco 2000	0.24	<1.20	2.0	0.12

[a] 3-arm star-branched polybutadiene; linking agent was CH_3SiCl_3. [b] 4-arm star-branched polybutadiene; linking agent was $SiCl_4$. [c] Molecular weights were obtained using $[\eta]_{TCB} = 4.86 \times 10^{-4} M^{0.705}$.[5] [d] Corrected values for the same samples reported in ref 3.

Table II
Solvents Used and Their Properties at 25 °C

solvent	sample code	η_{solv}, P	ρ_{solv}, g/cm³
Flexon 391[a]	F391	43.3	0.979
Flexon 340[a]	F340	0.73	0.954
Sundex 790[b]	S790	24.0	0.995
Philrich 5[c]	PH5	126.0	0.982
tetradecane	TD	0.021	0.763
low-$\bar{M}_w$ PB[d]	L3	6.4	0.900
isobutyl acetate	IBA		0.873

[a] Exxon Chemical Co. [b] Sun Oil Co. [c] Phillips Petroleum Co. [d] Sample 5L of ref 3.

polybutadiene solutions were prepared by dissolving polymer and wax in boiling cyclohexane and then precipitating rapidly by adding an excess of cold methanol. Separate studies confirmed complete precipitation of both components.

The dynamic storage and loss moduli, $G'(\omega)$ and $G''(\omega)$, were measured with a Rheometrics mechanical spectrometer using the eccentric rotating disk (ERD) geometry. Details of the procedure and precautions are described elsewhere[6,8] as are confirmations of such data by independently measured oscillatory data.[9] In one case (undiluted HPB-350) data were obtained by oscillatory methods alone because the ERD corrections for instrument compliance were too large. All measurements on the polybutadiene systems were made at 25 °C except for the isobutyl acetate solution (20 °C; $T \approx \Theta$). Measurements on the hydrogenated polybutadiene systems were made at 130 and 190 °C. Measurements on polystyrene were reduced by superposition procedures to 170 °C.[6] Measurements on polyisoprene and hydrogenated polyisoprene were made at 25 °C.[7]

Values of η_0 and J_e^0 were obtained with the standard linear viscoelastic relations[1]

$$\eta_0 = \lim_{\omega \to 0} \frac{G''(\omega)}{\omega} \tag{5}$$

$$J_e^0 = \frac{1}{\eta_0^2} \lim_{\omega \to 0} \frac{G'(\omega)}{\omega^2} \tag{6}$$

The hydrogenated polybutadiene systems did not reach the limiting storage modulus behavior,[5] so J_e^0 could not be obtained in those cases. The results are given in Tables III–V. Solvent viscosities were measured with calibrated Cannon-Ubbelohde capillary viscometers (Table II).

Procedures for Analyzing Dynamic Data

If the form of the terminal spectrum is universal for sufficiently long linear chains at high concentrations, the terminal spectrum for particular cases must be expressable as

$$H_1(\tau) = bH_1^*(\tau/a) \tag{7}$$

where H_1^* is the terminal spectrum in some convenient reference state and a and b are shift factors ($a = b = 1$ in the reference state) which depend on polymer and diluent species as well as T, M, and ϕ. Equations 1–3 yield the following relations:[10]

$$G_N^0 = b(G_N^0)^* \tag{8}$$

$$\eta_0 = ab(\eta_0)^* \tag{9}$$

$$J_e^0 = \frac{1}{b}(J_e^0)^* \tag{10}$$

from which it is clear that the product $G_N^0 J_e^0 = (G_N^0)^*(J_e^0)^*$ must be a universal constant if the terminal spectrum form is universal. Thus, the observation that $G_N^0 J_e^0$ for long linear chains is insensitive to M, ϕ, T, and species in consistent with the assumption of universality.

The dynamic moduli can be expressed in terms of the corresponding reference state functions and the same shift factors:[10]

$$G'(\omega) = b[G'(a\omega)]^* \tag{11}$$

$$G''(\omega) = b[G''(a\omega)]^* \tag{12}$$

It follows that the maximum in terminal loss modulus, G_m'', which is observed for linear chain systems and the frequency at the loss maximum, ω_m [$dG''/d\omega = 0$ at ω_m], are given by

$$G_m'' = b(G_m'')^* \tag{13}$$

$$\omega_m = (\omega_m)^*/a \tag{14}$$

Thus, $G_m''/G_N^0 = (G_m''/G_N^0)^*$ and $\eta_0\omega_m/G_N^0 = (\eta_0\omega_m/G_N^0)^*$ must also be universal constants if eq 7 is valid. The quantities G_N^0, G_m'', $1/J_e^0$, and $\omega_m\eta_0$ are proportional to the modulus shift factor b alone and so must vary with ϕ, M, and T in the same manner. Finally, from eq 11–14, the dynamic moduli plotted in reduced variables, G'/G_m'' and G''/G_m'', vs. ω/ω_m, must have universal forms:

$$\frac{G'(\omega/\omega_m)}{G_m''} = \left[\frac{G'(\omega/\omega_m)}{G_m''}\right]^* \tag{15a}$$

$$\frac{G''(\omega/\omega_m)}{G_m''} = \left[\frac{G''(\omega/\omega_m)}{G_m''}\right]^* \tag{15b}$$

Results on Linear Chain Systems

Loss modulus data for several undiluted linear polymer species ($M > M_c$) are plotted in Figure 1. Reduced variables, G''/G_m'' and ω/ω_m, are used. Values of G_m'' and ω_m for the samples are given in Table VI. According to the Ferry equation[1]

$$G_N^0 = \frac{2}{\pi}\int_{-\infty}^{\infty} G''(\omega)\, d \ln \omega \tag{16}$$

(terminal region only)

Table III
Rheological Properties of Linear Polybutadiene Solutions at 25 °C

sample	ϕ	η_0, P	ω_m, s^{-1}	J_e^0, cm^2/dyn	G_N^0, dyn/cm^2
L350 in F391	1.000	3.35×10^7	0.30	1.92×10^{-7}	1.18×10^7
	0.846	2.40×10^7	0.32	3.25×10^{-7}	7.27×10^6
	0.432	4.84×10^6	0.40	1.19×10^{-6}	1.78×10^6
	0.222	4.60×10^5	0.63	7.46×10^{-6}	2.89×10^5
	0.107	6.32×10^4	1.15	2.70×10^{-5}	7.27×10^4
	0.0854	3.40×10^4	1.60	4.64×10^{-5}	4.80×10^4
	0.0578	5.20×10^3	4.00	1.21×10^{-4}	1.96×10^4
	0.0325	1.16×10^3	8.70	2.90×10^{-4}	
	0.0126	3.20×10^2		3.44×10^{-4}	
L340 in TD	1.000	3.24×10^7	0.34	1.76×10^{-7}	1.32×10^7
	0.679	3.55×10^6	1.30	4.03×10^{-7}	4.91×10^6
	0.480	6.51×10^5	3.00	8.89×10^{-6}	2.30×10^6
	0.433	4.02×10^5	4.00	1.16×10^{-6}	1.83×10^6
	0.312	9.17×10^4	7.02	2.36×10^{-6}	8.35×10^5
	0.247	3.13×10^4	16.1	4.18×10^{-5}	4.91×10^5
	0.169	5.23×10^3	30.7	1.08×10^{-5}	1.87×10^5
L230 in F391	1.000	7.46×10^6	1.20	1.74×10^{-7}	1.15×10^7
	0.513	1.80×10^6	1.45	7.91×10^{-7}	2.64×10^6
	0.271	3.57×10^5		3.12×10^{-6}	6.78×10^5
L230 in L3	0.592	1.83×10^6	1.60	7.59×10^{-7}	3.56×10^6
	0.290	1.78×10^5		2.83×10^{-6}	6.94×10^5
L230 in IBA	0.431	1.39×10^5		1.14×10^{-6}	2.30×10^6
L230 in TD	0.855	2.45×10^6	3.30	2.97×10^{-7}	7.97×10^6
	0.656	6.69×10^5	7.00	5.06×10^{-7}	4.69×10^6
	0.476	1.25×10^5	16.0	9.93×10^{-7}	2.10×10^6
	0.409	6.34×10^4	25.0	1.32×10^{-6}	4.91×10^5
	0.345	3.80×10^4	28.5	2.22×10^{-6}	1.00×10^5
	0.256	8.53×10^3	63.0	3.64×10^{-6}	5.77×10^4
	0.189	1.91×10^3	101.0	7.72×10^{-6}	2.89×10^4
L200 in F391	1.000	5.41×10^6	2.00	1.80×10^{-7}	1.15×10^7
	0.420	7.00×10^5	2.14	1.34×10^{-6}	1.59×10^6
	0.242	1.28×10^5	3.40	4.36×10^{-6}	4.59×10^5
	0.161	3.44×10^4	5.25	1.15×10^{-5}	1.87×10^5
	0.108	8.43×10^3	9.12	2.53×10^{-5}	8.16×10^4
L200 in TD	0.361	5.49×10^4	26.9	2.00×10^{-6}	1.42×10^6
L200 in PH5	0.420	8.30×10^5	1.86	1.43×10^{-6}	1.52×10^6
L200 in F340	0.414	2.50×10^5	5.40		1.42×10^6
L200 in S790	0.424	5.00×10^5	2.50	1.80×10^{-6}	1.32×10^6

Table IV
Rheological Properties of Solutions of Linear Hydrogenated Polybutadienes

sample	ϕ	η_0(130 °C), P	η_0(190 °C), P	ω_m(130 °C), s^{-1}	G_N^0(130 °C), dyn/cm^2
HPB-350 in Bareco 1000	1.000	1.12×10^7	3.50×10^6	2.21	2.21×10^7
	0.826	7.00×10^6	2.05×10^6	2.61	1.50×10^7
	0.662	3.07×10^6	9.86×10^5	3.18	9.51×10^6
	0.498	1.54×10^6	4.94×10^5	4.00	5.91×10^6
	0.310	3.51×10^5	1.04×10^5	5.88	2.12×10^6
	0.211	8.32×10^4	2.46×10^4	8.82	7.72×10^5
	0.100	5.06×10^3	1.60×10^3	23.7	1.26×10^5
HPB-230 in Bareco 1000	1.00	2.34×10^6	7.20×10^5	9.64	2.06×10^7
	0.712	7.46×10^5	2.32×10^5	13.6	1.07×10^7
	0.401	1.22×10^5	3.75×10^4	22.4	3.10×10^6
PHPB-4 in Bareco 2000	1.000	7.80×10^5	2.39×10^5	37.3	2.65×10^7
	0.643	2.21×10^5	6.60×10^4	37.9	8.19×10^6
	0.335	3.10×10^4	8.80×10^3	61.9	1.99×10^6
PHPB-5 in Bareco 2000	1.000	1.76×10^6	5.54×10^5	14.2	2.29×10^7
	0.820	1.20×10^6	3.75×10^5	14.1	1.49×10^7

so, with the universal terminal spectrum hypothesis (eq 7), the area under the curve in Figure 1 should give, for sufficiently long chains, the universal proportionality constant K relating G_m'' and G_N^0:

$$\frac{G_N^0}{G_m''} = 2.303\left[\frac{2}{\pi}\int_{-\infty}^{\infty}\frac{G''(\omega/\omega_m)}{G_m''}\,d\log(\omega/\omega_m)\right] = K \tag{17}$$

For $\omega/\omega_m < 1$ the superposition of data for different species and molecular weights is uniformly excellent, but the curves differ at higher frequencies. The differences correlate strongly with separation from the transition region. Also, the superposition of the loss moduli data obtained for various polymer systems does not merely reflect conformance to the standard linear viscoelastic relation given in eq 5. The loss moduli deviate from this relation for values of $\omega/\omega_m > 0.1$, but the superposition continues

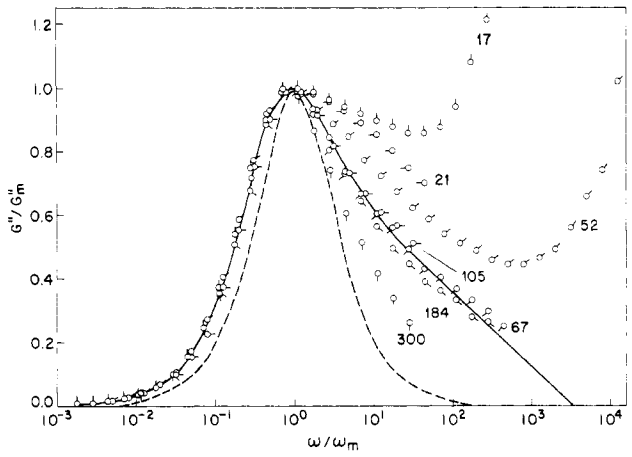

Figure 1. Reduced loss moduli curves for several narrow-distribution linear polymers. The various symbols denote G'' data on the polymers as follows: polystyrene at 170 °C, (◇) C6bb, (○) C7bb; polybutadiene at 25 °C, (○) L200, (○) L350; hydrogenated polybutadiene at 130 °C, (○) HPB-350; hydrogenated polyisoprene at 25 °C, (○) HPI-1; polyisoprene at 25 °C, (○) PI-1. The corresponding values of M/M_e are also shown. The solid curve represents the limiting behavior for long-chain ($M/M_e \approx 100$) linear polymers (Table VII) and the dashed line that of a single Maxwell element (eq 19).

Table V
Rheological Properties of Solutions of Star-Branched Polybutadienes at 25 °C

sample	ϕ	η_0, P	J_e^0, cm²/dyn
S200 in F391	1.000	9.50×10^7	1.29×10^{-6}
	0.812	1.38×10^7	1.50×10^{-6}
	0.609	1.45×10^6	2.07×10^{-6}
	0.403	1.15×10^5	3.30×10^{-6}
	0.206	8.62×10^3	6.54×10^{-6}
	0.108	1.04×10^3	1.45×10^{-5}
	0.0526	1.38×10^2	
S100 in F391	1.000	8.98×10^5	1.21×10^{-6}
	0.763	2.14×10^5	1.47×10^{-6}
	0.538	4.54×10^4	1.76×10^{-6}
	0.409	1.66×10^4	2.50×10^{-6}
	0.197	8.61×10^2	5.38×10^{-6}
	0.105	1.52×10^2	
	0.0533	9.90×10^1	
S200 in TD	0.656	4.02×10^5	2.05×10^{-6}
	0.405	6.66×10^3	3.45×10^{-6}

to be good even for values of $\omega/\omega_m \approx 1.0$. Values of the entanglement molecular weight were calculated for each species with[1]

$$M_e = \rho\phi RT/G_N^0 \tag{18}$$

for $\phi = 1$. Values of M/M_e are given in Table I for each sample. (If M/M_c were used, all values would be lower by a factor of approximately 2.[2]) The smooth progression of the curves with increasing M/M_e indicates a decrease in the overlap with plateau and transition contributions. Except for HPB, the data appear to converge to a limiting curve for $M/M_e \gtrsim 100$. The solid curve was drawn empirically through this region to represent what we tentatively conclude to be the asymptotic behavior for linear chain systems when $M \gg M_c$.

The HPB data were not used in establishing the limiting G'' curve because polyethylene melts appear to be somewhat nonrepresentative. Unlike other species the storage modulus G' is anomalous at low frequencies, and time–temperature superposition is violated in samples with long branches.[5] Also, the variations for $\omega/\omega_m > 1$ are less strongly dependent on dilution (decreasing M/M_e; see below) than in the other species. There are also some experimental difficulties in obtaining accurate values of G'' at high frequencies in undiluted HPB, owing to its unusually large plateau modulus.[9] Until such matters are cleared up, we prefer to omit the HPB data altogether in the establishment of limiting forms.

The loss modulus for a single relaxation time process (single Maxwell element)

$$\frac{G''}{G_m''} = 2\frac{\omega/\omega_m}{1 + (\omega/\omega_m)^2} \tag{19}$$

is shown by the dashed line in Figure 1. Although the limiting behavior (solid curve) corresponds to a narrow spectrum, it is still broader than a single-line spectrum, especially at high frequencies. There are some processes with relaxation times greater than $1/\omega_m$ and apparently a tail of shorter relaxation time processes extending even below $0.1/\omega_m$. On the other hand, although all samples have narrow molecular weight distributions, some broadening must also be caused by sample polydispersity.

It is somewhat surprising that molecular weights corresponding to $M/M_e \approx 100$ (or $M/M_c \approx 50$) are required to eliminate plateau and transition relaxations from the terminal behavior. The separation between transition and terminal relaxations goes roughly as $(M/M_c)^{3.4}$ so overlap with transition region processes, whose contributions are presumably independent of chain length (for $M > M_c$), should decrease much more rapidly than this. The results strongly suggest that intermediate processes are involved, such as, for example, the equilibration step of the Doi–Edwards model.[11] Such processes might shift with chain length, but less rapidly than true terminal processes, and might therefore be more accurately described as plateau relaxations.

The area under the limiting curve in Figure 1 gives, with eq 17

$$G_N^0 = 3.56G_m'' \tag{20}$$

This result is somewhat different from the Marvin–Oser equation, $G_N^0 = 4.83G_m''$, which is based on a shifted Rouse model for the terminal spectrum.[1] Values of G_N^0 calculated with eq 20 are given in Table VI for the various species.

Table VI
Rheological Properties of Undiluted Polymers

sample	η_0, P	J_e^0, cm²/dyn	G_N^0, dyn/cm²	ω_m, s⁻¹	$\eta_0\omega_m/G_N^0$	$J_e^0G_N^0$
L200	5.41×10^6	1.80×10^{-7}	1.15×10^7	2.0×10^0	0.94	2.07
L350	3.35×10^7	1.92×10^{-7}	1.18×10^7	3.0×10^{-1}	0.85	2.27
HPB-350[a]	1.12×10^7		2.21×10^7	2.2×10^0	1.11	
PI-1[b]	5.75×10^5	6.30×10^{-7}	3.26×10^6	5.6×10^0	0.99	2.05
HPI-1[c]	2.97×10^7	1.99×10^{-7}	1.13×10^7	3.6×10^{-1}	0.95	2.25
C6bb[d]	3.10×10^6	1.20×10^{-6}	1.78×10^6	5.6×10^{-1}	0.98	2.14
C7bb[d]	1.50×10^8	1.25×10^{-6}	1.78×10^6	1.1×10^{-2}	0.93	2.23

[a] HPB data shown were collected at 130 °C. [b] Polyisoprene data at 25 °C were obtained from ref 7. [c] Hydrogenated polyisoprene data at 25 °C were obtained from ref 7. [d] Polystyrene data at 170 °C were obtained from ref 6.

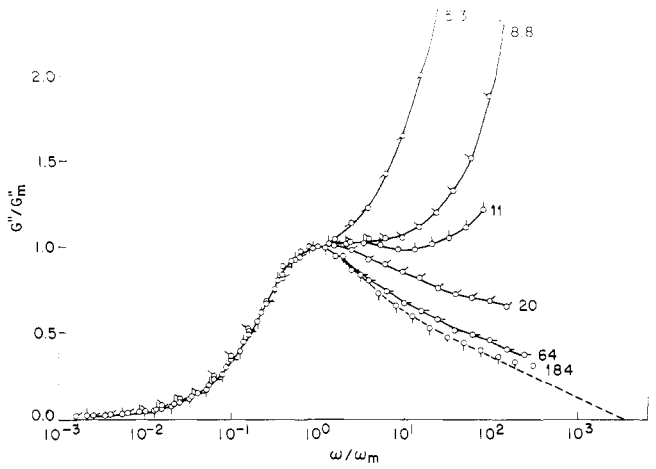

Figure 2. Reduced loss moduli curves for polybutadiene solutions (sample L350 in F391) at 25 °C. The symbols denote volume fraction of polymer: (○) 1.000; (○) 0.432; (○) 0.222; (○) 0.107; (○) 0.0854; (○) 0.0578. The dashed line represents the limiting behavior obtained for undiluted high molecular weight linear polymers in Figure 1. The values of M/M_e shown were calculated with eq 18.

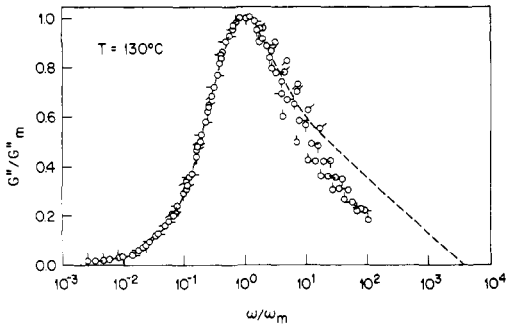

Figure 3. Reduced loss moduli curves for hydrogenated polybutadiene solutions (sample HPB-350 in Bareco 1000) at 130 °C. The symbols denote volume fraction of polymer: (○) 1.000; (○) 0.828; (○) 0.662; (○) 0.498; (○) 0.310; (○) 0.211. The dashed line has the same meaning as in Figure 2.

The changes from earlier values are small except for polystyrene, which is reduced about 12%, and HPB, which is increased about 5%. Equation 20, of course, only applies to data on linear polymers with very narrow molecular weight distributions and $M > M_c$.

Figures 2 and 3 show similar reduced plots for solutions of polybutadiene and hydrogenated polybutadiene. The pattern is similar to that in Figure 1. Superposition is good for $\omega/\omega_m < 1$ and in excellent accord with the data in Figure 1, but at higher frequencies the curves in Figure 2 differ systematically with M/M_c (altered by dilution in this case). For $\omega/\omega_m < 1$ the HPB data (Figure 3) are indistinguishable from the polybutadiene data. Values for G_N^0 calculated from G_m'' with eq 20 are given in Tables III and IV for the solutions.

Figure 4 shows reduced plots of storage moduli for the undiluted polymers in Figure 1. Superposition is again uniformly good for $\omega/\omega_m < 1$ except for HPB, which departs at the lowest frequencies, as mentioned earlier. The solid curves are estimates of the limiting terminal response. Values of G'/G_m'' and G''/G_m'' vs. ω/ω_m from these curves are given in Table VII. From these limiting curves, the following universal values ($M/M_e \geq 100$) were obtained:

$$G_N^0 J_e^0 = 2.40 \quad (21)$$

$$\eta_0\omega_m/G_N^0 = 0.97 \quad (22)$$

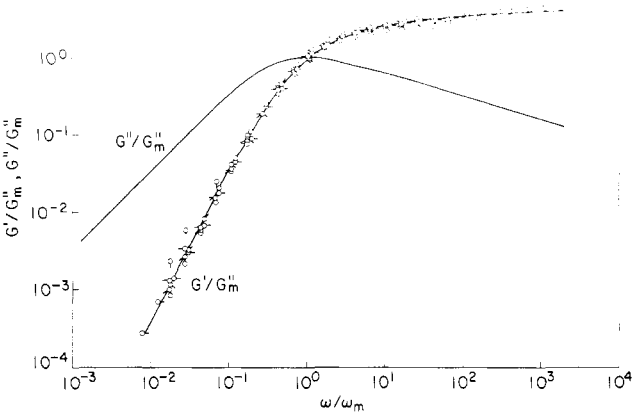

Figure 4. Reduced storage moduli for several narrow-distribution linear polymers. The symbols and the solid lines have the same meaning as in Figure 1. The solid lines represent the limiting behavior for long-chain linear polymers (Table VII).

Table VII
Universal Reduced Dynamic Storage and Loss Moduli for Narrow-Distribution Polymers

$\log(\omega/\omega_m)$	$\log(G'/G_m'')$	$\log(G''/G_m'')$
−2.80		−2.30
−2.60		−2.10
−2.40		−1.90
−2.20	−3.82	−1.70
−2.00	−3.42	−1.49$_5$
−1.80	−3.02	−1.29
−1.60	−2.64	−1.08
−1.40	−2.26	−0.87
−1.20	−1.87	−0.68
−1.00	−1.48	−0.50
−0.80	−1.15	−0.33
−0.60	−0.81	−0.19
−0.40	−0.50	−0.07$_5$
−0.20	−0.24$_5$	−0.02
0.00	−0.05	0.00
0.20	0.09$_5$	−0.02
0.40	0.21	−0.06
0.60	0.28$_5$	−0.11
0.80	0.36$_5$	−0.15$_5$
1.00	0.40	−0.20$_5$
1.20	0.43	−0.25$_5$
1.40	0.46$_5$	−0.30
1.60	0.49	−0.34$_5$
1.80	0.50$_5$	−0.39$_5$
2.00	0.52$_5$	−0.44$_5$
2.20	0.54	−0.50$_5$
2.40	0.55	−0.58
2.60	0.56	−0.66
2.80	0.57	−0.77
3.00	0.58	−0.90$_5$
3.20	0.59	−1.12$_5$

In general, we find that $G'(\omega)$ and $G''(\omega)$ settle into their limiting forms rather quickly for $\omega < \omega_m$ ($M \approx 5M_e$). Much larger values of M/M_e are required to resolve the limiting terminal forms at higher frequencies. Thus, properties such as G_m'', $\eta_0\omega_m$, and J_e^0, which are independent of or insensitive to moduli for $\omega > \omega_m$, assume their limiting dependencies on variables such as volume fraction of polymer substantially before the full resolution ($M/M_e \approx 100$) is attained. in Figure 5 the values of plateau modulus for polybutadiene solutions (Table III) are plotted as a function of ϕ for various solvents and molecular weights. Except for a constant factor ($G_N^0 = 3.56G_m''$) this is equivalent to plotting G_m'' vs. ϕ. Irrespective of molecular

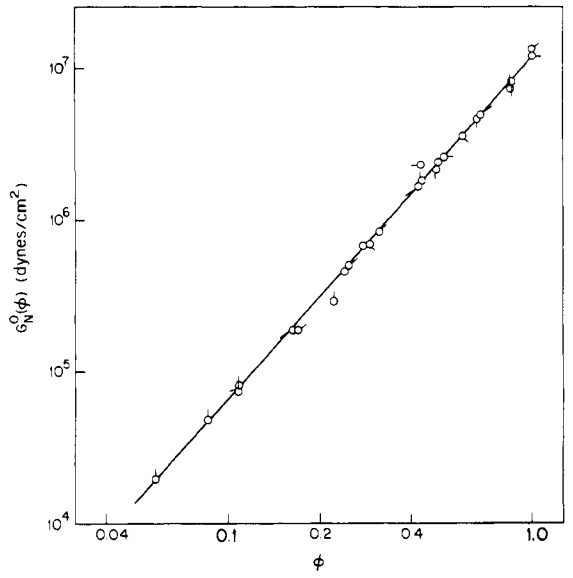

Figure 5. Plateau moduli as a function of volume fraction of polymer for polybutadiene solutions in different solvents: (◊) L350 in F391; (○) L340 in TD; (○) L230 in F391; (□) L230 in L3; (○) L230 in TD; (○) L230 in IBA; (□) L200 in F391.

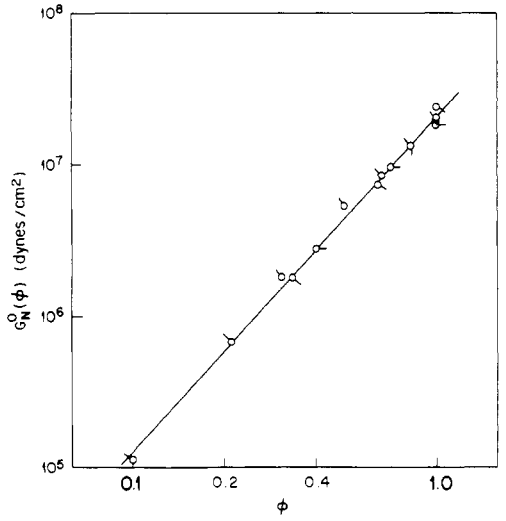

Figure 6. Plateau moduli as a function of ϕ for hydrogenated polybutadiene solutions at 130 °C: (○) HPB-350 in Bareco 1000; (○) HPB-230 in Bareco 1000; (□) PHPB-4 in Bareco 2000; (○) PHPB-5 in Bareco 2000.

weight and the solvent species, the data obey a simple power law relation over the entire range of concentration:

$$G_N^0 = 1.18 \times 10^7 \phi^{2.26} \quad \text{(polybutadiene)} \quad (23)$$

A similar result is obtained in Figure 6 for hydrogenated polybutadiene solutions (Table IV):

$$G_N^0 = 2.11 \times 10^7 \phi^{2.22} \quad \text{(hydrogenated polybutadiene)} \quad (24)$$

Values of J_e^0 for the polybutadiene solutions (Table III) are plotted in Figure 7. Above $\phi = 0.05$ the data obey the relation

$$J_e^0 = 1.81 \times 10^{-7} \phi^{-2.24} \quad \text{(polybutadiene)} \quad (25)$$

Figures 8 and 9 show $\eta_0\omega_m$ vs. ϕ for the polybutadiene and hydrogenated polybutadiene solutions. The results are

$$\eta_0\omega_m = 1.05 \times 10^7 \phi^{2.22} \quad \text{(polybutadiene)} \quad (26)$$

$$\eta_0\omega_m = 2.55 \times 10^7 \phi^{2.30} \quad \text{(hydrogenated polybutadiene)} \quad (27)$$

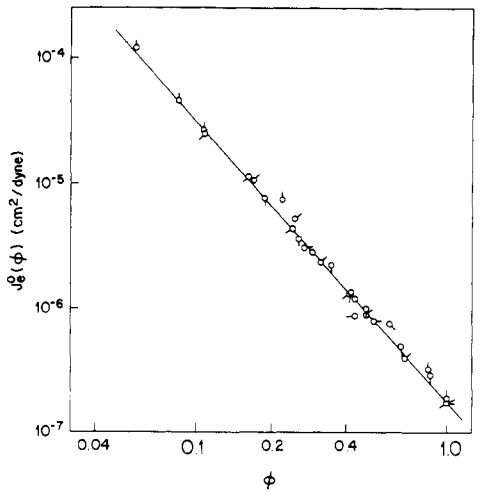

Figure 7. Steady-state recoverable compliance as a function of ϕ for polybutadiene solutions at 25 °C. The symbols have the same meaning as in Figure 5.

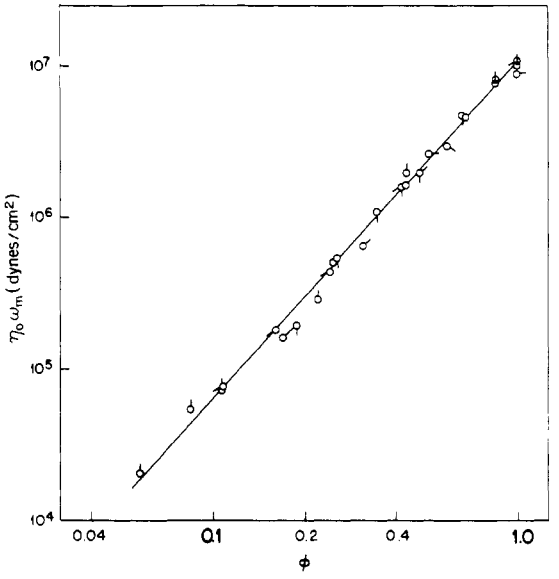

Figure 8. $\eta_0\omega_m$ vs. log ϕ for polybutadiene solutions. The symbols have the same meaning as in Figures 5 and 7.

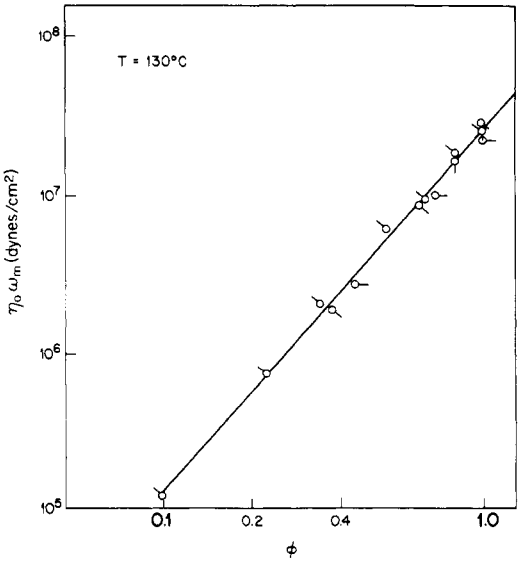

Figure 9. $\eta_0\omega_m$ vs. log ϕ for hydrogenated polybutadiene solutions in low molecular weight linear polyethylenes. The symbols have the same meaning as in Figure 6.

Combinations of eq 23–27 give (for $\phi = 1$)

$$\eta_0\omega_m/G_N^0 = 0.89 \quad \text{(polybutadiene)}$$

$$\eta_0\omega_m/G_N^0 = 1.21 \quad \text{(hydrogenated polybutadiene)}$$

$$J_e^0 G_N^0 = 2.14 \quad \text{(polybutadiene)}$$

and negligible variations with molecular weight, solvent species, and volume fractions. Values of these groups for the other polymers are given in Table VI, showing only slight variations with polymer species and good numerical consistency with eq 21 and 22. Interestingly, even though hydrogenated polybutadiene departs from the other polymers in the behavior of G' at low frequencies, its agreement with eq 22 is still rather good.

The concentration dependence of the modulus shift factor b has been discussed elsewhere.[3] The results here, based on $\eta_0\omega_m$ as well as G_m'' (or G_N^0) and J_e^0 values, support an isothermal dependence which is slightly stronger than quadratic ($b \propto \phi^{2.25}$) for polybutadiene and polyethylene. Analysis of recent results on polystyrene solutions[12,13] suggests a slightly weaker dependence ($b \propto \phi^{2.1}$)[14] but data at different dilutions in these cases were obtained at widely different temperatures and hence required also a separate temperature reduction. Isothermal studies of J_e^0 on blends of high molecular weight polystyrene in low molecular weight polystyrene ($M < M_c$) in fact suggest $b \propto \phi^{2.3}$.[15] Assumptions that G_N^0 is proportional to the concentration of binary contacts between chain segments lead to a quadratic dependence, $b \propto \phi^2$, in systems which are unperturbed by excluded volume effects. Scaling arguments suggest $b \propto \phi^{2.25}$ for the good solvents in the semidilute region.[16] The latter exponent is closer to some of the above observations, but the experimental results (Figures 5–9) are independent of solvent power (see also ref 17), and the larger exponent applies experimentally right up to the undiluted state. Both of these characteristics are inconsistent with scaling argument expectations. Nevertheless, it would certainly be useful to obtain more complete data on Θ solvent systems and perhaps to combine all such experiments with measurements of chain dimensions over the full range of concentrations.

Results on Star-Branched Systems

Figures 10 and 11 show storage and loss modulus data for several concentrations of the 4-arm star polybutadiene S200 in F391. Both G' and G'' exhibit the conventional behavior at low frequencies ($G' \propto \omega^2$; $G'' \propto \omega$) in all the star solutions. Values of η_0 and J_e^0 were obtained with eq 5 and 6 and are given in Table V. The dynamic moduli rise much more gradually with increasing frequency than in linear polymers, however, and the prominent maximum in G'', characteristic of linear polymer systems, is entirely absent. The same behavior is observed for the three-arm star S100. The terminal spectrum in long-arm stars is clearly much broader than in the comparable linear species, and it extends to much shorter times.

The absence of a loss modulus maximum (at least in the accessible range of frequencies) and the extension of terminal contributions to very high frequencies obviate the use of eq 16 to determine G_N^0. There is some evidence, however, suggesting that G_N^0 is the same for linear and long-branched systems. A loss maximum is observed at high frequencies in long-arm polystyrene stars, and the G_N^0 obtained (from eq 16) is the same as for linear polystyrene.[6] The topological contribution to the equilibrium modulus of networks, G_e^{max}, is closely related to plateau modulus,[18] and G_e^{max} was found to be the same for polybutadiene networks formed by cross-linking either linear chains or

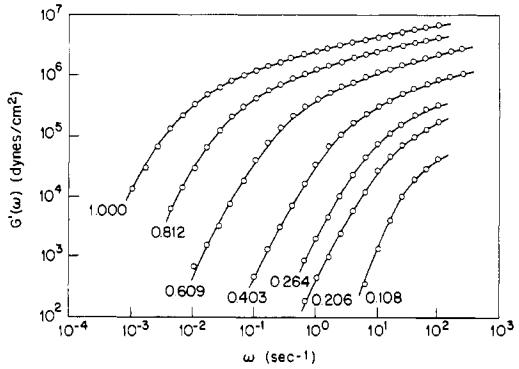

Figure 10. Dynamic storage moduli curves for solutions of 4-arm star-branched polybutadiene sample S200 in F391. The volume fraction of polymer is shown for each solution.

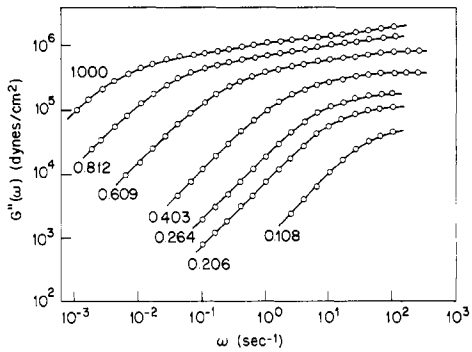

Figure 11. Dynamic loss moduli curves for solutions of the sample S200 in F391.

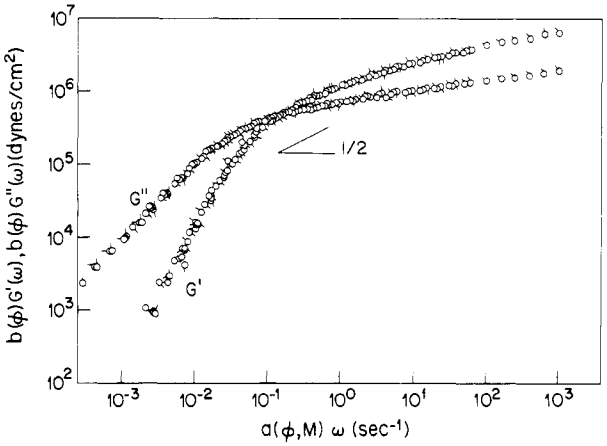

Figure 12. Reduced dynamic moduli curves for the sample S200 in F391. The symbols denote volume fraction of polymer: (○) 1.000; (○) 0.812; (○) 0.609; (○) 0.403; (○) 0.264; (○) 0.203; (○) 0.108.

stars.[19] However, the data in Figures 10 and 11 could not be superposed by shifting along the frequency axis if a modulus shift factor proportional to $\phi^{-2.26}$ (eq 23) was imposed. On the other hand, excellent superposition was obtainable by allowing the shift factors to vary arbitrarily. The results are shown in Figures 12 and 13. Undiluted polymer was the reference state in each case; the values of $a(\phi)$ and $b(\phi)$ are listed for each polymer in Table VIII.

Figure 14 shows the modulus shift factor as a function of concentration. Values of b were obtained from the modulus shift which produced the best superposition (Table VIII), from the recoverable compliance (eq 10), and from the frequency shift and the viscosity (eq 9 and 14). There is a certain amount of redundancy among the three methods to estimate b, but even so, the agreement is

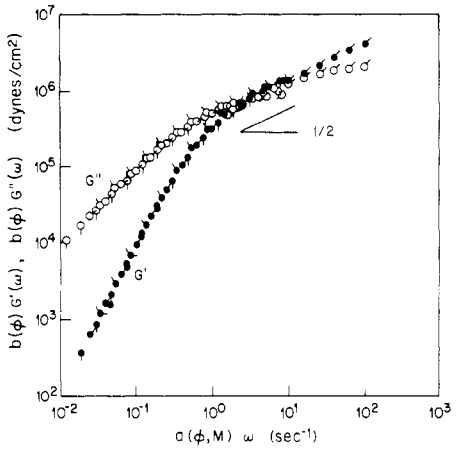

Figure 13. Reduced dynamic moduli curves for the 3-arm star-branched polybutadiene sample S100 in F391. The open symbols denote loss moduli and the filled symbols storage moduli with volume fractions of polymer (○) 1.000, (○) 0.538, (○) 0.409, and (○) 0.197.

Table VIII
Shift Factors $a(\phi)$ and $b(\phi)$ for Star-Branched Polymer Solutions in F391

ϕ	log $a(\phi)$	log $b(\phi)$
	Sample S200	
1.0	0.0	0.0
0.812	−0.79	0.06
0.609	−1.65	0.17
0.403	−2.57	0.34
0.206	−3.14	0.54
0.108	−3.38	0.72
0.0526	−3.95	1.01
	Sample S100	
1.0	0.0	0.0
0.538	−1.11	0.18
0.409	−1.46	0.3
0.197	−2.32	0.7

gratifying. The concentration dependence of the modulus shift factor is clearly weaker than in the case of linear polybutadienes, and, to within experimental error, $b = \phi$ for stars (reference state: undiluted polymer).

The contrast in behavior of long linear chains and long-arm stars is further illustrated in Figure 15. The recoverable compliance for polybutadiene solutions is plotted in reduced form[2]

$$J_{eR} = \frac{J_e^0 \rho \phi RT}{g_2 M}\left[\frac{\eta_0}{\eta_0 - \eta_s}\right]^2 \tag{28}$$

as a function of M/M_e, where values of M_e at each concentration are calculated from eq 18 and 23, η_s is the solvent viscosity, and

$$g_2 = (15f - 14)/(3f - 2)^2 \tag{29}$$

for f-arm stars. Agreement with results from the Rouse–Ham model[20] corresponds to $J_{eR} = 0.4$. For $M/M_e \lesssim 6$ both linear and star polymers are in substantial agreement with the Rouse–Ham equation. The linear polymers depart strongly beyond $M/M_e = 6$, and $J_{eR} \propto (M/M_e)^{-1}$, reflecting their stronger concentration dependence and independence of molecular weight in this range (eq 25). The stars, however, continue along the Rouse–Ham line, showing very small departures, if any, over the entire range. It is evident, however, that the form of the spectrum is quite different from that predicted by the Rouse–Ham model. In the latter G' and G'' are both proportional to $\omega^{1/2}$ at intermediate frequencies and G'' is always greater

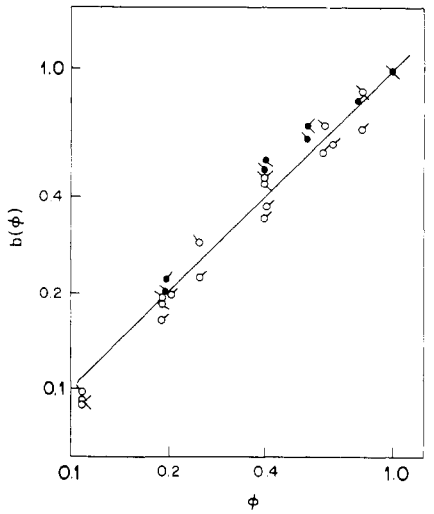

Figure 14. Vertical shift factors as a function of volume fraction of polymer for star-branched polybutadiene solutions. The open symbols denote solutions of the sample S100 and the filled symbols the sample S200; values of $b(\phi)$ obtained from (○) $\eta_0/a(\phi)$, (○) vertical shifts in Figures 12 and 13, and (○) steady-state compliance values.

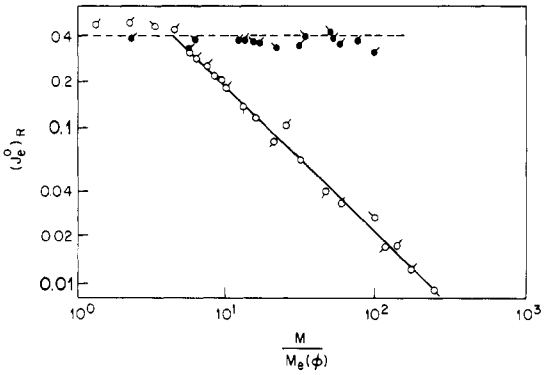

Figure 15. Reduced compliance as a function of M/M_e for linear and star-branched polybutadiene solutions in F391. Filled symbols denote star-branched polymers: (●) S200; (●) S100. Open symbols denote linear polymers: (○) L200; (○) L230; (○) 350; (○) L500; (○) L700. The broken line shows the prediction obtained from the Rouse–Ham model and the solid line is drawn with a slope of −1.

than G',[1] which is clearly not the case in Figures 12 and 13.

The point was made earlier that in the long-chain limit $J_e^0 G_N^0$ should be a universal constant if the terminal spectrum can be expressed by eq 7. That appears to be the case for linear chain systems. For long-arm stars dynamic moduli data at different concentrations are consistent with eq 7. However, $J_e^0 \propto \phi^{-1}$ for stars, and we have been assuming that $G_N^0 \propto \phi^k$, where k is 2 or greater, irrespective of the large-scale structure. The implied inconsistency is removed, however, when it is recalled that the terminal spectrum is much broader for stars and that we have been able to examine only the properties of the leading edge (the long-time region). For linear chains the separation from other processes even on the trailing edge (short-time end) of the terminal spectrum becomes more or less complete when $M/M_e \approx 100$. The separation is incomplete in the stars because the trailing edge is so greatly attenuated. If the separation could be accomplished, it might well be found that G_N^0 goes approximately as ϕ^2 and J_e^0 as ϕ^{-1} but that eq 7 is not literally valid over the entire terminal spectrum: the spectrum for stars might settle into a universal form in the leading edge but con-

tinue to change at the trailing edge, even for stars with very long arms.

Conclusions

We have shown that the terminal relaxation spectrum for linear chains approaches a limiting form at high molecular weights and concentrations ($M/M_e \gg 1$). The limiting form at the long-time end appears to be attained rather quickly ($M/M_e \approx 5$), but values of $M/M_e \approx 100$ seem necessary to resolve the part at short times. An estimate of reduced dynamic moduli for the fully resolved terminal spectrum was made. Values of the universal constants $J_e^0 G_N^0 = 2.4$, $G_N^0/G_m'' = 3.56$, and $\eta_0\omega_m/G_N^0 = 0.97$ were derived from the limiting curves and found to be in good agreement with the values for different species and concentrations. The modulus shift factor varies with concentration as $b \propto \phi^k$, where k is somewhat greater than 2. The behavior of stars differs substantially. Dynamic moduli for stars at different concentrations can be superposed, but the modulus shift factor has a much weaker concentration dependence: $b \propto \phi$. Assuming $G_N^0 \propto \phi^k$ for both linear and star polymers, $J_e^0 G_N^0$ for stars is a function of concentration, molecular weight, and polymer species. Thus, the terminal spectrum for star polymers appears not to approach constant limiting form, at least in the range of compositions investigated here.

Acknowledgment. This work was supported by the National Science Foundation (Grant ENG 77-15683-A01 to Northwestern University and Grant DMR-79-08299 to the University of Akron). We thank the Northwestern University Materials Research Center for use of its facilities. We are also grateful to Mr. Jeffrey Gotro of Northwestern University and Dr. Jacques Roovers of the National Research Council of Canada for permission to use their data.

References and Notes

(1) Ferry, J. D. "Viscoelastic Properties of Polymers", 3rd ed.; Wiley: New York, 1980.
(2) Graessley, W. W. *Adv. Polym. Sci.* **1974**, *16*, 1.
(3) Marin, G.; Menezes, E. V.; Raju, V. R.; Graessley, W. W. *Rheol. Acta* **1980**, *19*, 462.
(4) Rochefort, W. E.; Smith, G. G.; Rachapudy, H.; Raju, V. R.; Graessley, W. W. *J. Polym. Sci., Part A-2* **1979**, *17*, 1197.
(5) Raju, V. R.; Rachapudy, H.; Graessley, W. W. *J. Polym. Sci., Part A-2* **1979**, *17*, 1223.
(6) Graessley, W. W.; Roovers, J. *Macromolecules* **1979**, *12*, 959.
(7) Gotro, J., private communication.
(8) Raju, V. R.; Smith, G. G.; Marin, G.; Knox, J. R.; Graessley, W. W. *J. Polym. Sci., Part A-2* **1979**, *17*, 1183.
(9) Vrentas, C. M.; Rochefort, W. E.; Smith, G. G.; Graessley, W. W. *Polym. Eng. Sci.* **1981**, *21*, 285.
(10) Markovitz, H. *J. Polym. Sci., Polym. Symp.* **1975**, *50*, 431. Plazek, D. J.; Riande, E.; Markovitz, H. Raghupathi, N. *J. Polym. Sci., Part A-2* **1979**, *17*, 2189.
(11) Doi, M.; Edwards, S. F. *J. Chem. Soc., Faraday Trans. 2* **1978**, *74*, 1789, 1802, 1818.
(12) Isono, Y.; Fujimoto, T.; Takeno, N.; Kajiura, H.; Nagasawa, M. *Macromolecules* **1978**, *11*, 888.
(13) Riande, E.; Markovitz, H.; Plazek, D. J.; Raghupathi, N. *J. Polym. Sci., Polym. Symp.* **1975**, *50*, 405.
(14) Graessley, W. W., manuscript in preparation.
(15) Orbon, S. J.; Plazek, D. J. *J. Polym. Sci., Part A-2* **1979**, *17*, 1871.
(16) Daoud, M.; Cotton, J. P.; Farnoux, B.; Jannink, G.; Sarma, G.; Benoit, H.; Duplessix, R.; Picot, C.; de Gennes, P. G. *Macromolecules* **1975**, *8*, 804.
(17) Isono, Y.; Nagasawa, M. *Macromolecules* **1980**, *13*, 862.
(18) Dossin, L. M.; Graessley, W. W. *Macromolecules* **1979**, *12*, 123.
(19) Dossin, L. M. Ph.D. Thesis, Materials Science and Engineering Department, Northwestern University, Evanston, Ill., 1978.
(20) Rouse, P. E. *J. Chem. Phys.* **1973**, *21*, 272. Ham, J. S. *Ibid.* **1957**, *26*, 625.

Influence of Flow on the Isotropic–Nematic Transition in Polymer Solutions: A Thermodynamic Approach

T. J. Sluckin*

Department of Mathematics, University of Bristol, University Walk, Bristol BS8 1TW, United Kingdom. *Received February 26, 1981*

ABSTRACT: The effect of an elongational flow field on the concentration dependence of the isotropy–anisotropy transition in dilute polymers is investigated by a quasi-thermodynamic method. It is found that in such flow fields the transition is shifted toward the low-concentration regime. The shift depends on a number of experimentally accessible quantities in the bulk phases. The resulting equations have a Clausius–Clapeyron-like form.

Introduction

Polymers which consist of rigid rodlike sections can, under some circumstances, in sufficiently concentrated solutions, exist in an anistropic nematic phase. This can be important in achieving high-modulus properties. In general, at low concentrations the nematic phase does not form. However, at some critical polymer mole fraction c_I a nematic phase at polymer mole fraction $c_N > c_I$ can be in equilibrium with the isotropic phase at mole fraction c_I. Homogeneous solutions with polymer mole fraction c, where $c_I < c < c_N$, cannot exist; rather the solution separates into two homogeneous phases with different polymer mole fractions c_I and c_N. A basic statistical mechanical theory of this phenomenon was developed by Flory.[1]

In view of the possible technological significance of these anisotropic solutions, it is of interest to ask what circumstances might favor the formation of the anisotropic phase. One such circumstance is to place the polymer solution in an extensional flow field. It has been known for some time[2,3] that flow fields can have significant orientation effects. Marrucci and Sarti[4] investigated the effect of elongational flow on the isotropy–anisotropy transition. They used a quasi-equilibrium statistical mechanical approach, assuming irrotational flow and, thus, that the velocity field was describable in terms of a potential, and they modeled the polymer in solution by a freely jointed

* Present address: Faculty of Mathematical Studies, University of Southampton, Highfield, Southampton, SO9 5NH, United Kingdom.

0024-9297/81/2214-1676$01.25/0